



# Investigation of SiO<sub>2</sub> Nanoparticle Reinforced Epoxy Composites Produced by Additive Manufacturing: Effect of Silanization on Conversion Degree and Mechanical Properties

Berk Özler<sup>1,a,\*</sup>, Serdar Yıldırım<sup>2,b</sup>

<sup>1</sup> Department of Metallurgical and Materials Engineering, University of Izmir Katip Celebi, 35620, Izmir, Türkiye

<sup>2</sup> Department of Metallurgical and Materials Engineering, University of Dokuz Eylül, 35390, Izmir, Türkiye

\*Corresponding author

## Research Article

### History

Received: 09/01/2025

Accepted: 01/03/0025

### Copyright



This work is licensed under  
Creative Commons Attribution 4.0  
International License

## ABSTRACT

3D printers have revolutionized many areas such as aviation, dentistry, health, construction, food, pharmacy and tissue engineering by forming the basis of additive manufacturing technology. These devices, which work by adding material layer by layer, combine with CAD software to enable the rapid and efficient production of complex designs. DLP printers in the photochemical category stand out in medical applications by polymerizing photosensitizer resins with UV light. While inorganic fillers in these resins increase mechanical properties, excessive use can increase viscosity and reduce printing performance. Although SiO<sub>2</sub> nanoparticles increase transparency and durability, their tendency to clump negatively affects mechanical properties. By coating the surface of these particles with the silanization method, they are better bonded with the resin, thus improving the integrity and mechanical strength of the structure. In this study, the aim is to investigate the effects of the silanization process on the mechanical properties and conversion degree of particles in epoxy composite materials reinforced with SiO<sub>2</sub> nanoparticles. For this purpose, nanoparticles synthesized by the sol-gel method and subjected to the silane coating process were added to the epoxy resin at different rates and produced with a DLP type 3D printer. In the study, critical parameters such as the compatibility of coated and uncoated nanoparticles with the resin matrix, the viscosity properties of the material, mechanical strength and conversion degree were evaluated with detailed analyses. The highest conversion degree increase (24.4%) occurred in the 2 wt.% silane-coated SiO<sub>2</sub> sample. The 1 wt.% silane-coated SiO<sub>2</sub> sample showed the greatest tensile strength (66.4%), and modulus increase (10.5%), while the 2 wt.% silane-coated SiO<sub>2</sub> sample had the highest flexural strength increase (5.1%). The obtained results revealed the effect of silane coating on increasing the performance of the material.

**Keywords:** Additive manufacturing, nanocomposite, silanization, mechanical properties, conversion degree.

## Araştırma Makalesi

### Süreç

Geliş: 09/01/2025

Kabul: 01/03/0025

## ÖZ

3D yazıcılar, eklemeli üretim teknolojisinin temelini oluşturarak havacılık, diş hekimliği, sağlık, inşaat, gıda, eczacılık ve doku mühendisliği gibi birçok alanda devrim yaratmıştır. Malzemeyi katman katman ekleyerek çalışan bu cihazlar, CAD yazılımlarıyla birleşerek karmaşık tasarımların hızlı ve verimli bir şekilde üretilmesini sağlamaktadır. Fotokimyasal kategorideki DLP yazıcılar, fotosensitör reçinelerini UV ışığıyla polimerize ederek tıbbi uygulamalarda öne çıkmaktadır. Bu reçinelerdeki inorganik dolgular mekanik özellikleri artırırken, aşırı kullanımı viskoziteyi artırarak baskı performansını düşürebilmektedir. SiO<sub>2</sub> nanopartikülleri şeffaflığı ve dayanıklılığı artırmaya rağmen, topaklanma eğilimleri mekanik özellikleri olumsuz etkilemektedir. Bu partiküllerin yüzeyinin silanizasyon yöntemi ile kaplanmasıyla reçineyle daha iyi bağlanmaları sağlanmakta, böylece yapının bütünlüğü ve mekanik mukavemeti artmaktadır. Bu çalışmada, SiO<sub>2</sub> nanopartikülleri ile takviye edilmiş epoksi kompozit malzemelerde silanizasyon işleminin partiküllerin mekanik özellikleri ve dönüşüm derecesi üzerindeki etkilerinin incelenmesi amaçlanmıştır. Bu amaçla sol-jel yöntemi ile sentezlenen ve silan kaplama işlemine tabi tutulan nanopartiküller farklı oranlarda epoksi reçinesine eklenerek DLP tipi 3D yazıcı ile üretilmiştir. Çalışmada, kaplanmış ve kaplanmamış nanopartiküllerin reçine matrisi ile uyumluluğu, malzemenin viskozite özellikleri, mekanik mukavemet ve dönüşüm derecesi gibi kritik parametreler detaylı analizlerle değerlendirilmiştir. En yüksek dönüşüm derecesi artışı (%24,4) ağırlıkça %2 silan kaplı SiO<sub>2</sub> içeren numunede meydana gelmiştir. Ağırlıkça %1 silan kaplı SiO<sub>2</sub> içeren numune ise çekme mukavemetinde (%66,4) ve elastisite modülünde (%10,5) en iyi artışı göstermiştir. Ağırlıkça %2 silan kaplı SiO<sub>2</sub> içeren numunenin ise en yüksek eğilme mukavemeti artışına (%5,1) sahip olduğu görülmüştür. Elde edilen sonuçlar, silan kaplamanın malzemenin performansını artırma etkisini ortaya koymuştur.

**Anahtar Kelimeler:** Eklemeli imalat, nanokompozit, silanizasyon, mekanik özellikler, dönüşüm derecesi..

berk.ozler@ikcu.edu.tr

0000-0003-1819-6032

serdar.yildirim@deu.edu.tr

0000-0002-3730-3473

**How to Cite:** Ozler B, Yıldırım S. (2023) Investigation of SiO<sub>2</sub> Nanoparticle Reinforced Epoxy Composites Produced by Additive Manufacturing: Effect of Silanization on Conversion Degree and Mechanical Properties, Journal of Science and Technology, 4(1): 12-20.

## Introduction

In recent years, 3D printers have become highly regarded and influential within the field of additive manufacturing technology. These cutting-edge devices have transformed the production of intricate and complex geometric designs, surpassing traditional methods like casting and machining. Since their emergence in the 1980s, 3D printers have attracted significant attention due to their exceptional ability to produce multiple objects simultaneously (Chen et al., 2019). The additive manufacturing process they utilize involves layering material sequentially from a starting point on a platform to create three-dimensional objects. This process is repeated until the final product is complete. Essentially, this technology represents a robotic adaptation of age-old manufacturing practices, akin to building a brick wall. By leveraging CAD (Computer-Aided Design) software, 3D printers play a crucial role in designing and fabricating detailed three-dimensional models (Horvath, 2014). Advancements in the field have significantly broadened the potential applications of 3D printers in recent years. Their improved efficiency, sustainability, and accelerated production capabilities, in alignment with the principles of Industry 4.0, have enabled their adoption across a range of disciplines, including arts, civil construction, food, healthcare, aerospace, dentistry, the pharmaceutical industry, tissue engineering and biomaterials (A. L. Silva, Salvador, Castro, Carvalho, & Munoz, 2021; Zhang & Xiao, 2018).

Three-dimensional printers can be classified according to their manufacturing methods, which include photochemical, electrical, and mechanical processes. DLP (Digital Light Processing) printers, which fall into the photochemical category, have become extremely common, especially in medical applications. These types of printers use ultraviolet (UV) light to photopolymerize photosensitive resins that shape the final product. The main constituents of these resins are oligomers, monomers, and photoinitiators. In certain instances, color pigments and fillers (nano and/or microparticles) might also be included (Zhang & Xiao, 2018). Photoinitiators drive the photopolymerization process, creating a polymer through cross-linking. The conversion degree and mechanical properties of a polymer are directly influenced by these cross-links. Additionally, incorporating inorganic fillers into the resin structure can increase the strength and density of cross-links, further enhancing the conversion degree and mechanical properties of the material (Aati, Akram, Ngo, & Fawzy, 2021; Al-Turaif, 2010; N. Bahremandi Tolou, M. H. Fathi, A. Monshi, V. S. Mortazavi, & M. Mohammadi, 2013; Pehlivan & Karacaer, 2014). However, in addition to this improvement, inorganic fillers can increase the viscosity of the resin and, when exceeded to a certain level, may have negative effects on printability material (Bao, Paunović, & Leroux, 2022).

In medical applications, such as dentistry and tissue engineering, achieving a high conversion degree and superior mechanical properties are crucial. A key strategy to enhance these properties is the dispersion of SiO<sub>2</sub> nanoparticles (NPs) within the resin matrix. These NPs are highly valued for their outstanding mechanical attributes and their ability to maintain the transparency of resin (Rezvani, Atai, Hamze, &

Hajrezai, 2016). However, a significant limitation of SiO<sub>2</sub> NPs is their tendency to agglomerate, which reduces the effective surface area in contact with the resin and negatively impacts mechanical properties (Pehlivan & Karacaer, 2014). To overcome this issue, silanization is employed. Silanization is a process of applying silane groups to the particle surfaces. This coating prevents NP aggregation and promotes better bonding with the resin matrix, reinforcing overall structural integrity (Neibloom, Bevan, & Frechette, 2020; Nguyen et al., 2020; Tham, Chow, & Ishak, 2010).

In this study, silane-coated and uncoated SiO<sub>2</sub>-reinforced epoxy matrix nanocomposites were produced using a DLP type 3D printer. The mixtures were prepared in different ratios with and without coating. The viscosities of the prepared resins were examined, and the printing process was initiated. Comprehensive characterization tests were carried out on the materials before and after the printing process. The effect of the silanization process applied to the NPs in the structure on conversion degree and mechanical properties was investigated.

## Material and Method

The SiO<sub>2</sub> NPs utilized in the present study were synthesized via a sol-gel method, employing tetraethylorthosilicate (TEOS) as the starting material. Ethanol (EtOH) and ammonia (NH<sub>3</sub>) were utilized as organic solvent and catalyst, respectively. Ammonia was incorporated into the solution prepared by adding TEOS to EtOH with the objective of accelerating the gelation process. Subsequently, the solution was stirred and aged at room temperature until it became gel. The obtained gel was then dried at 250 °C and calcined at 600 °C to yield the desired NP product. Subsequently, the silanization process of the synthesized powders was carried out using 3-(trimethoxysilyl)propylmethacrylate (MPS). The obtained powders were mixed by incorporating them into a solution containing ethanol (EtOH) and MPS. During the mixing process, ammonia was added to the solution with MPS to enhance the bonding of organic structures to the SiO<sub>2</sub> NP surface. The resultant powders, which were stirred at room temperature for 24 hours, were then subjected to a centrifugation method to precipitate the desired material. Subsequent to this step, the powders were purified from the solution using EtOH, followed by drying at 70 °C, thereby completing the silane coating process.

Photosensitive epoxy resin (Standard Resin, AnyCubic) was utilized as the matrix material for the composite materials under investigation. Coated (C) and uncoated (U) NPs were incorporated into the resin at ratios of 0% (Pure), 0.5%, 1%, 2%, and 5% by weight. The contents and acronyms of the nanocomposites obtained are listed in Table 1. The mixture was thoroughly blended using a magnetic stirrer. Following the attainment of a homogeneous distribution, the printing process was executed using a DLP type 3D printer (Halot-Sky CL89, Creality). Layer thickness and exposure time, referred to as printing parameters, were set to 50 µm and 5 s, respectively, ensuring consistency across all samples. After printing, each composite was subjected to a cleaning procedure involving an isopropyl alcohol bath in a washer

and curing device (UW-02, Creality). Then, the composites were exposed to a post-curing process under UV light for a duration of one hour.

*Table 1. Acronyms and contents of the nanocomposites.*

Name	Uncoated SiO <sub>2</sub> (wt. %)	Name	Coated SiO <sub>2</sub> (wt. %)
U5	0.5	C5	0.5
U10	1	C10	1
U20	2	C20	2
U50	5	C50	5

Structural and thermal properties of the synthesized SiO<sub>2</sub> NPs were determined by an X-ray diffractometer (XRD) and thermogravimetric analysis (TGA), respectively. Cu-K $\alpha$  radiation (1.5406 Å) was used in the XRD measurement (ARL X'TRA, Thermo Scientific) in order to acquire diffraction patterns for a 2 $\theta$  value. For all samples, XRD data were obtained at a scan rate of 2 °/min within the 10° $\leq$ 2 $\theta$  $\leq$ 80° range. TGA (STA 8000, PerkinElmer) was performed in N<sub>2</sub> atmosphere by heating at a rate of 10 °/min to a temperature of 800 °C. Organic bond structures and conversion degrees of NPs and composites were ascertained through the use of Fourier transform infrared spectroscopy (FTIR) and their morphological properties were determined using scanning electron microscopy (SEM). FTIR (Nicolet iS10, Thermo Scientific) analysis was performed with 32 scans for each sample in the range of 500 to 4000 cm<sup>-1</sup> wavenumber. SEM (Gemini 560, Zeiss) images were obtained using secondary electron mode at 5 kV voltage with the magnification of 50K and 100K for NPs, back-scattered electron mode at 15 kV voltage with the magnification of 5K for composites. Viscosity properties of the Pure and composite resins were measured by a rheometer (CVO Rheometer System, Bohlin Instruments). The measurement was executed using the cone and plane method, employing a cone with a 2° angle and maintaining a 100  $\mu$ m distance between the planes. The shear rate range was configured within the range of 0 to 1000 1/s, and measurements were obtained at room temperature for a duration of 120 seconds. The mechanical properties of the composite samples were determined by performing tensile (AG-IS, Shimadzu) and three-point bending (AG-50kNG, Shimadzu) tests. Three specimens were used for testing and an average value of the results was used. In both tests, the speed was set to 1 mm/min, and cylindrical

supports were used as spans with a span-to-depth ratio of 16:1 in the three-point bending test.

## Results and Discussion

### Particle Characterization

The structural and thermal properties of the NPs were determined by TGA and XRD. The temperature-dependent weight loss (%) for the produced SiO<sub>2</sub> xerogel is demonstrated in Figure 1a. A detailed examination of the graph reveals that the weight loss between 70 and 150 °C corresponds to the removal of water and moisture, and the weight loss between 180 °C and 550 °C corresponds to the combustion of organic components such as alkyl groups (-CH<sub>2</sub>CH<sub>3</sub>) and the removal of -OH groups from SiOH (Zornoza-Indart & López-Arce, 2015). Given the absence of phase transition in the structure and the occurrence of linear weight loss from 600 °C, it was considered reasonable to execute the calcination process of the synthesized particles at this temperature.

The X-ray diffraction (XRD) profile of the synthesized SiO<sub>2</sub> NPs is shown in Figure 1b. The broad dominant peak obtained as a result of the analysis indicates that the derived SiO<sub>2</sub> NPs are amorphous because they do not exhibit a crystalline structure, and the lack of any additional peaks in the spectrum indicates that there are no impurities from the synthesis process, resulting in a pure composition (Varshney, Nigam, Pawar, & Mishra, 2022), (Dubey, Rajesh, & More, 2015).

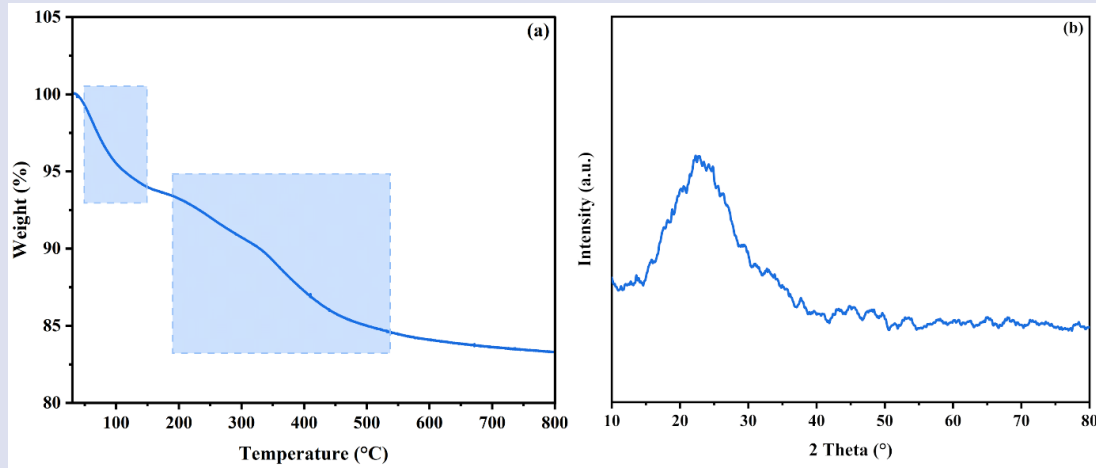


Figure 1. Thermogravimetric analysis (a) and X-ray diffractometer analysis (b) of SiO<sub>2</sub> xerogel and NPs, respectively.

### Morphological Properties

The morphological properties of NPs and composites were investigated by SEM analysis. The examination of NP samples was conducted in secondary electron mode, while composites were analyzed using backscattered electron mode. Representative images of NPs and composites at 50K and 100K magnifications for NPs and 5K magnification for composites are presented in Figure 2.

In order to ascertain their true shape and size, SEM analysis of the NPs was carried out before the silanization process. The examination of Figure 2a and 2b, images reveal the presence of particle agglomeration. Upon further examination of the sizes of small particles within agglomerated particles, it was revealed that there are spherical particles randomly distributed in the range of 40 - 100 nm. The composite samples, comprising both uncoated and coated samples with a 1% SiO<sub>2</sub> additive (designated as U10 and C10, respectively), were subjected to examination from the cross-sectional area. The presence of SiO<sub>2</sub> NPs is indicated by white dots in the matrix material. A comparison of the images reveals that the particles are predominantly in large clusters in Figure 2c and in smaller clusters and a single structure in Figure 2d. It was observed that the silane-coated

samples exhibited a behavior consistent with the findings reported in the extant literature (Mussatto, Oliveira, Subramani, Papaléo, & Mota, 2020; Rossi Canuto de Menezes et al., 2021).

### Viscosity Properties

The viscosity properties of pure and composite resins were determined by rheometer measurement, and the obtained results are presented in Figure 3 and Table 2. Upon examination of these values, it was observed that NP addition generally increased viscosity, while silane-coated particles increased it even more than uncoated particles. Since the viscosity values remained constant at the measured shear rate, no thixotropic or non-Newtonian behavior was observed. A subsequent comparison of the findings with the extant literature revealed their consistency with the results reported in a study by Mohsen and Craig. The silane-coated samples exhibited enhanced interaction with the matrix material, attributable to the presence of organic compounds on their surfaces, thereby reducing fluidity (Mohsen & Craig, 1995).

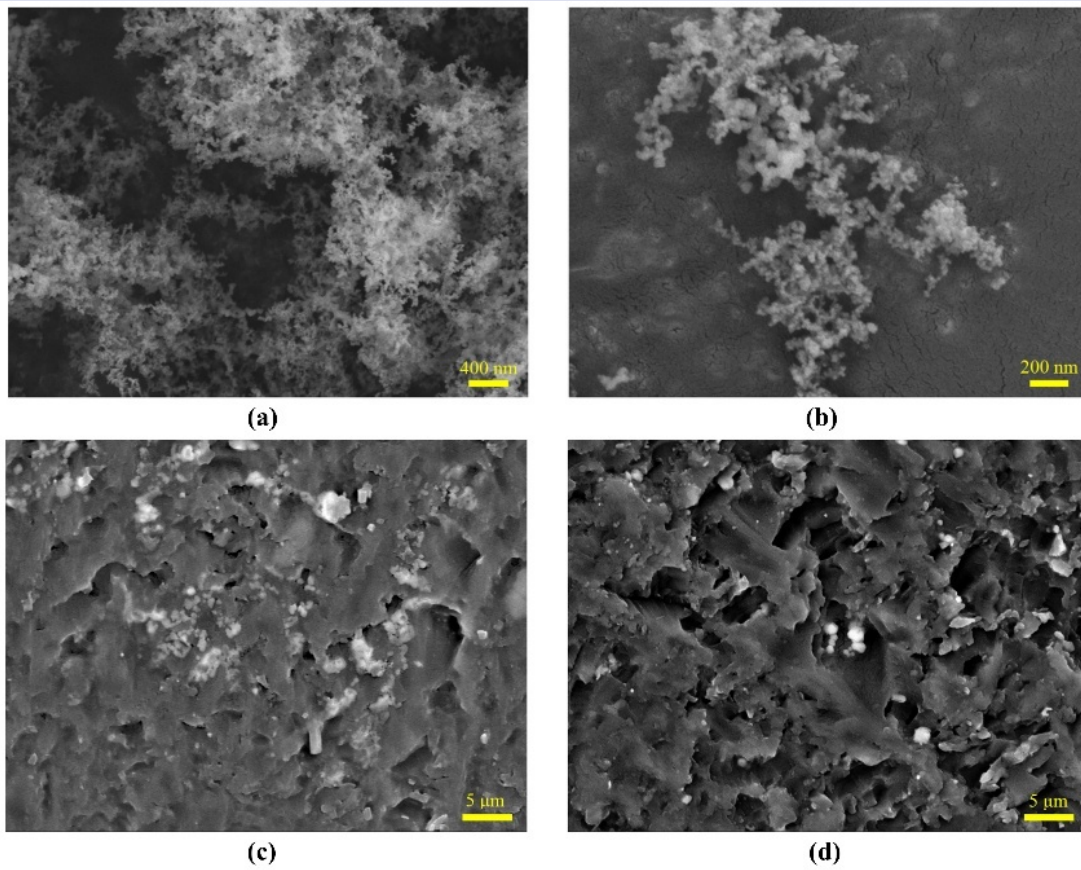


Figure 2. SEM images of SiO<sub>2</sub> NPs and composites. NPs at (a) 50K and (b) 100K magnification, and (c) U10 and (d) C10 samples at 5K magnification.

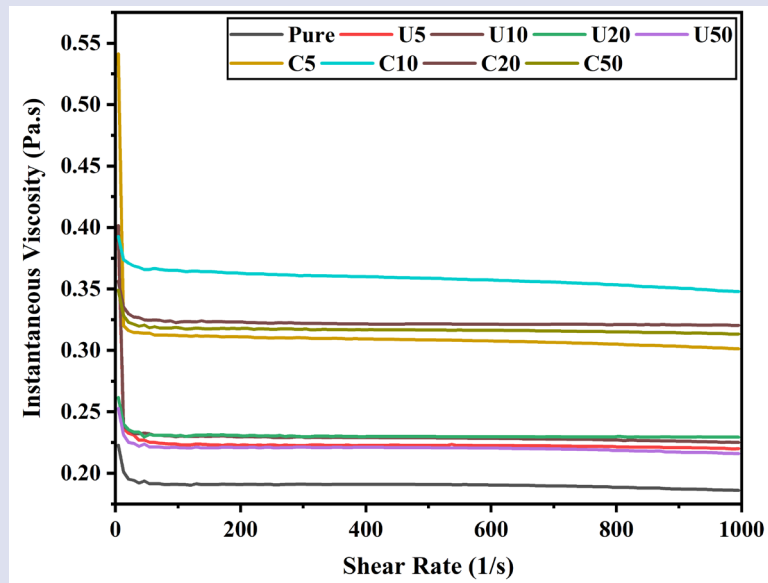


Figure 3. Instantaneous viscosities against shear rate of pure and composite resins.

Table 2. Instantaneous viscosity values of pure and composite resins.

Name	Viscosity (Pa.s)	Name	Viscosity (Pa.s)
Pure	0.19	C5	0.3
U5	0.22	C10	0.35
U10	0.23	C20	0.32
U20	0.23	C50	0.31
U50	0.22		

**Organic Bond Properties**

FTIR analysis of the NPs was conducted to ascertain the modifications in organic bond structure that occurred due to silanization. The FTIR spectra of uncoated and coated particles are presented in Figure 4. Upon examination of the graph, peaks at wave numbers of 1046 and 795 cm<sup>-1</sup>, which are common to both spectra, were identified. These peaks are known to correspond to Si-O-Si stretching and O-Si-O bending bonds, respectively. Consequently, the presence of these peaks is expected in both samples. (Moncada, Quijada, & Retuert, 2007) (see Figure 4). Upon zooming in on the graph, it was determined that the peak at the shared wave number of 1633 cm<sup>-1</sup> originated from the hydroxyl groups trapped in the SiO<sub>2</sub> structure and could also overlap with the C=C vibration in the MPS structure (Rong, Chen, Wu, & Wang, 2005; Siddiquey, Ukaji, Furusawa, Sato, & Suzuki, 2007). The peaks at 1455 and 1716 cm<sup>-1</sup> were identified as belonging to the C-H stretching and C=O vibration, respectively, within the MPS structure (Nguyen et al., 2020). The successful silanization process was confirmed through the identification of these bonds via FTIR analysis.

The conversion degrees of pure and composite resins following polymerization were determined by FTIR analysis, with the analysis applied to each sample before and after polymerization for the conversion degree calculation. The conversion degree calculation enables the determination of the polymerization capabilities of the materials by calculating the conversion rate of C=C double bonds in their structures to C-C single bonds as a result of cross-linking of monomers. The conversion degree calculation was carried out by using Equation

(1) given in Barszczewska-Rybarek's study (Barszczewska-Rybarek, 2012).

$$DC = 1 - \left( \frac{A_{C=C(t)}}{A_{C=C(o)}} \right) \times 100 \tag{1}$$

In the equation, A<sub>C=C</sub> is the intensity of the peak that corresponds to the C=C double bond at 1637 cm<sup>-1</sup> wavenumber, as can be seen in Figure 5a. The symbols (0) and (t) next to the A<sub>C=C</sub> are used to denote the intensity values of this peak before and after polymerization, respectively. The conversion degrees of pure and composite samples, as calculated according to Equation 1, are presented in Figure 6.

As demonstrated in Figure 5b, the silanization process exhibited a considerable positive impact on the conversion degree. It is hypothesized that this phenomenon leads to an enhancement in the conversion degree through the formation of bonds between the silane groups present on the NP surface and the acrylate groups embedded within the resin matrix during the polymerization process. This increased bonding facilitates the formation of additional crosslinks, contributing to an overall increase in the conversion degree. Among the composite samples, the highest increases were observed in C5 and C20 samples, with 23.8% and 24.4% increases, respectively. The observed decrease in the conversion degree of the U20 sample is hypothesized to be attributed to the restriction of polymerization resulting from NP agglomeration (Sodagar, Bahador, Khalil, Saffar Shahroudi, & Zaman Kassaei, 2013).

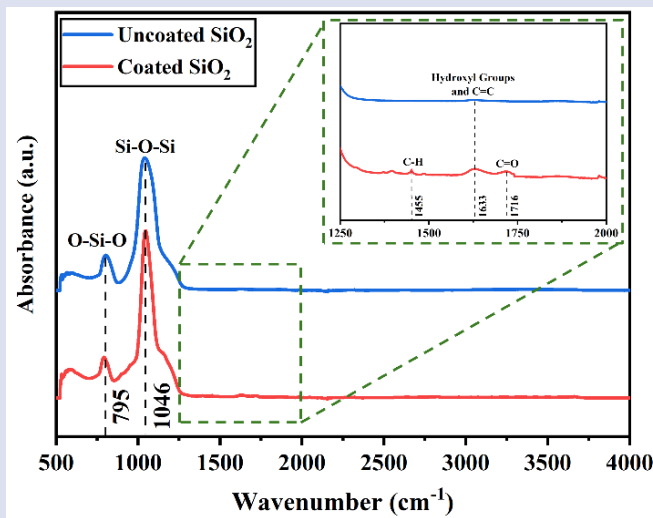


Figure 4. FTIR spectrum of uncoated and coated SiO<sub>2</sub> NPs.

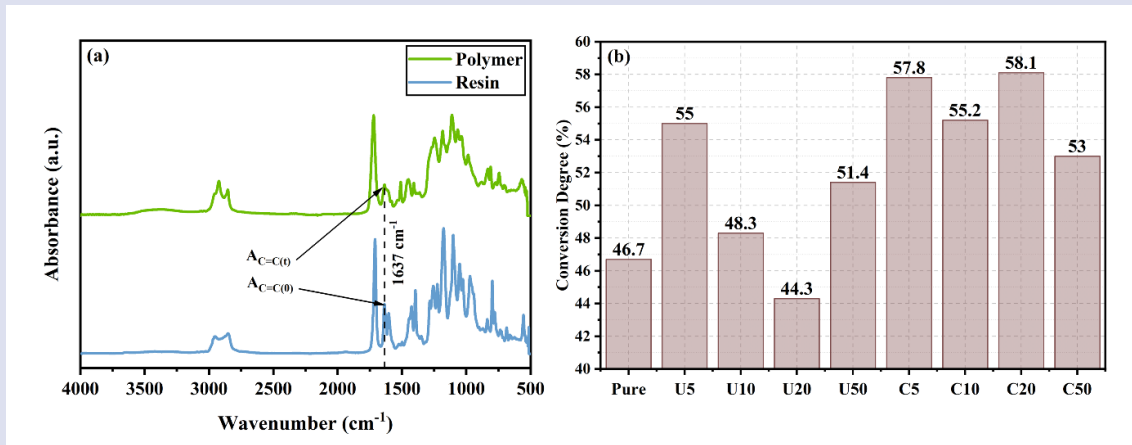


Figure 5. (a) FTIR spectrum of pure sample before and after polymerization and (b) conversion degrees of pure and composite samples.

### Mechanical Properties

Tensile and three-point bending tests were applied to determine the strengths of pure and composite materials. Tensile and flexural strength values are shown in Figures 6a and 6b, respectively, while Figure 6c shows the modulus of elasticity values obtained by the tensile test. In addition, the results are presented in comprehensive detail in Table 3. A general observation indicates that the effect of SiO<sub>2</sub> NP reinforcement on strength values up to 0.5 wt.% is positive. However, as the ratios increase, the strength value begins to decrease. This observation is consistent with the findings reported in the study by Da Silva et al. (L. H. da Silva, Feitosa, Valera, de Araujo, & Tango, 2012), which showed that the addition of SiO<sub>2</sub> has a positive impact on the mechanical properties up to a certain extent. However, in samples containing silane-coated NPs, a general increase occurred compared to uncoated samples and this increase continued

up to 2%. It was also confirmed by Gad et al. that this increase in mechanical properties occurred as a result of the reduction of stress concentration regions within the structure due to the silanization process reducing agglomeration (Gad et al., 2020). However, a decrease in strength values occurs after 2 wt.% silane-coated SiO<sub>2</sub> NP content. This situation caused a decrease in mechanical properties as the agglomeration of NPs increased again with the additions made after 2%.

The enhancement of mechanical properties is directly proportional to the conversion degree. As the cross-links in the structure are covalent bonds, and the number of these bonds increases, the network structure becomes denser, resulting in more homogeneous energy distribution within the material. This also reduces crack formation and propagation, thereby increasing the material's resistance to mechanical forces (Huang et al., 2022).

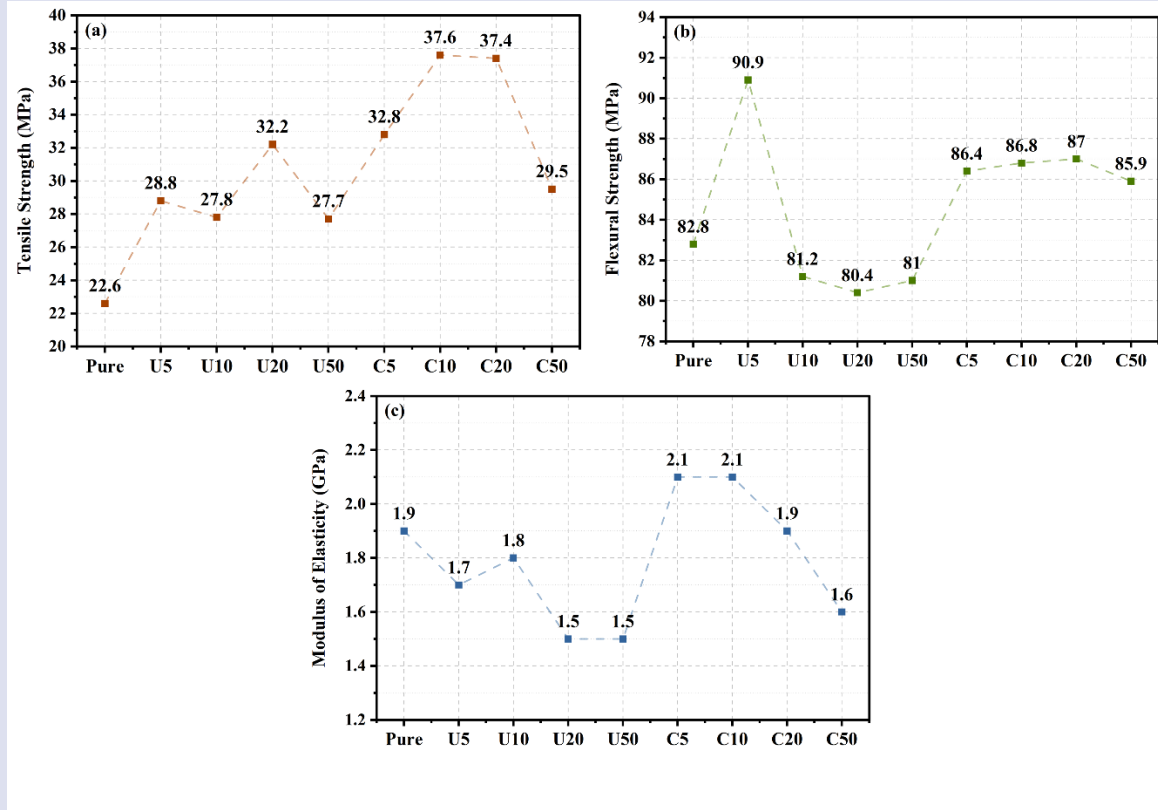


Figure 6. (a) Tensile strength, (b) flexural strength and (c) modulus of elasticity of pure and composite samples.

Table 3. Detailed tensile strength, flexural strength and modulus of elasticity values of pure and composite samples.

Name	Tensile Strength (MPa)	Flexural Strength (MPa)	Modulus of Elasticity (GPa)
Pure	22.6 ± 0.34	82.8 ± 0.69	1.9 ± 0.12
U5	28.8 ± 0.29	90.9 ± 0.42	1.7 ± 0.11
U10	27.8 ± 0.35	81.2 ± 0.45	1.8 ± 0.07
U20	32.2 ± 0.11	80.4 ± 0.4	1.5 ± 0.05
U50	27.7 ± 0.82	81 ± 0.34	1.5 ± 0.07
C5	32.8 ± 0.12	86.4 ± 0.18	2.1 ± 0.11
C10	37.6 ± 0.54	86.8 ± 0.26	2.1 ± 0.14
C20	37.4 ± 0.66	87 ± 0.69	1.9 ± 0.12
C50	29.5 ± 0.44	85.9 ± 0.18	1.6 ± 0.09

**Conclusion**

A comprehensive investigation has been conducted on the effect of silanization on SiO<sub>2</sub>-reinforced epoxy composite materials, with notable success. The synthesis by the sol-gel method and silane coating of NPs have been successfully achieved. The composite resins, obtained by varying the NP-to-matrix ratio during the addition process, were printed using a 3D printer. The findings of the study indicated that the silane coating process applied to the added NPs had a positive effect on the mechanical properties and conversion degree. The study's potential for enhancement was identified as follows: by using various matrix materials and NPs. This is particularly relevant in the domains of tissue engineering and

dentistry, where the enhancement of mechanical properties and the conversion degree through silanization of reinforcement materials in composite resins can lead to significant improvements.

**Acknowledgement**

This study was financially supported by Dokuz Eylul University, Scientific Research Projects Coordinatorship with the project code 2021.KB.FEN.046.

## References

- Aati, S., Akram, Z., Ngo, H., & Fawzy, A. S. (2021). Development of 3D printed resin reinforced with modified ZrO<sub>2</sub> nanoparticles for long-term provisional dental restorations. *Dental Materials*, 37(6), e360–e374. <https://doi.org/10.1016/j.dental.2021.02.010>
- Al-Turaif, H. A. (2010). Effect of nano TiO<sub>2</sub> particle size on mechanical properties of cured epoxy resin. *Progress in Organic Coatings*, 69(3), 241–246. <https://doi.org/10.1016/j.porgcoat.2010.05.011>
- Bao, Y., Paunović, N., & Leroux, J.-C. (2022). Challenges and opportunities in 3D printing of biodegradable medical devices by emerging photopolymerization techniques. *Advanced Functional Materials*, 32(15), 2109864. <https://doi.org/10.1002/adfm.202109864>
- Barszczewska-Rybarek, I. M. (2012). Quantitative determination of degree of conversion in photocured poly(urethane-dimethacrylate)s by Fourier transform infrared spectroscopy. *Journal of Applied Polymer Science*, 123(3), 1604–1611. <https://doi.org/10.1002/app.34553>
- Chen, Z., Li, Z., Li, J., Liu, C., Lao, C., Fu, Y., ... He, Y. (2019). 3D printing of ceramics: A review. *Journal of the European Ceramic Society*, 39, 661–687. <https://doi.org/10.1016/j.jeurceramsoc.2018.11.013>
- da Silva, L. H., Feitosa, S. A., Valera, M. C., de Araujo, M. A. M., & Tango, R. N. (2012). Effect of the addition of silanated silica on the mechanical properties of microwave heat-cured acrylic resin. *Gerodontology*, 29(2), e1019–e1023. <https://doi.org/10.1111/j.1741-2358.2011.00604.x>
- Dubey, R. S., Rajesh, Y. B. R. D., & More, M. A. (2015). Synthesis and characterization of SiO<sub>2</sub> nanoparticles via sol-gel method for industrial applications. *Materials Today: Proceedings*, 2(4), 3575–3579. <https://doi.org/10.1016/j.matpr.2015.07.098>
- Gad, M. M. A., Abualsaud, R., Al-Thobity, A. M., Almaskin, D. F., Alzahr, Z. A., Abushowmi, T. H., ... Al-Harbi, F. A. (2020). Effect of SiO<sub>2</sub> nanoparticles addition on the flexural strength of repaired acrylic denture base. *European Journal of Dentistry*, 14(1), 19–23. <https://doi.org/10.1055/s-0039-1701076>
- Horvath, J. (2014). A brief history of 3D printing. In *Mastering 3D printing* (pp. 3–10). Apress. [https://doi.org/10.1007/978-1-4842-0025-4\\_1](https://doi.org/10.1007/978-1-4842-0025-4_1)
- Huang, J., Fu, P., Li, W., Xiao, L., Chen, J., & Nie, X. (2022). Influence of crosslinking density on the mechanical and thermal properties of plant oil-based epoxy resin. *RSC Advances*, 12(36), 23048–23056. <https://doi.org/10.1039/D2RA04206A>
- Mohsen, N. M., & Craig, R. G. (1995). Effect of silanation of fillers on their dispersability by monomer systems. *Journal of Oral Rehabilitation*, 22(3), 183–189.
- Moncada, E., Quijada, R., & Retuert, J. (2007). Nanoparticles prepared by the sol-gel method and their use in the formation of nanocomposites with polypropylene. *Nanotechnology*, 18(33), 335606. <https://doi.org/10.1088/0957-4484/18/33/335606>
- Mussatto, C. M. B., Oliveira, E. M. N., Subramani, K., Papaléo, R. M., & Mota, E. G. (2020). Effect of silica nanoparticles on mechanical properties of self-cured acrylic resin. *Journal of Nanoparticle Research*, 22(11). <https://doi.org/10.1007/s11051-020-05050-y>
- Bahremandi Tolou, N., Fathi, M. H., Monshi, A., Mortazavi, V. S., & Mohammadi, M. (2013). The effect of adding TiO<sub>2</sub> nanoparticles on dental amalgam properties. *Iranian Journal of Materials Science and Engineering*, 10(2), 46–56. <http://ijmse.iust.ac.ir/article-1-565-en.html>
- Neibloom, D., Bevan, M. A., & Frechette, J. (2020). Surfactant-stabilized spontaneous 3-(trimethoxysilyl) propyl methacrylate nanoemulsions. *Langmuir*, 36(1), 284–292. <https://doi.org/10.1021/acs.langmuir.9b03412>
- Nguyen, T. C., Nguyen, T. D., Vu, D. T., Dinh, D. P., Nguyen, A. H., Ly, T. N. L., ... Thai, H. (2020). Modification of titanium dioxide nanoparticles with 3-(trimethoxysilyl)propyl methacrylate silane coupling agent. *Journal of Chemistry*, 2020, 1–9. <https://doi.org/10.1155/2020/1381407>
- Pehlivan, N., & Karacaer, Ö. (2014). Diş hekimliğinde kullanılan kompozit rezinlerin güçlendirilmesi. *Acta Odontologica Turcica*, 31, 160–166. <https://doi.org/10.17214/aot.66166>
- Rezvani, M. B., Atai, M., Hamze, F., & Hajrezai, R. (2016). The effect of silica nanoparticles on the mechanical properties of fiber-reinforced composite resins. *Journal of Dental Research, Dental Clinics, Dental Prospects*, 10(2), 112–117. <https://doi.org/10.15171/joddd.2016.018>
- Rong, Y., Chen, H. Z., Wu, G., & Wang, M. (2005). Preparation and characterization of titanium dioxide nanoparticle/polystyrene composites via radical polymerization. *Materials Chemistry and Physics*, 91(2–3), 370–374. <https://doi.org/10.1016/j.matchemphys.2004.11.042>
- Rossi Canuto de Menezes, B., da Graça Sampaio, A., Morais da Silva, D., Larissa do Amaral Montanheiro, T., Koga-Ito, C. Y., & Patrocínio Thim, G. (2021). AgVO<sub>3</sub> nanorods silanized with γ-MPS: An alternative for effective dispersion of AgVO<sub>3</sub> in dental acrylic resins improving the mechanical properties. *Applied Surface Science*, 543, 148830. <https://doi.org/10.1016/j.apsusc.2020.148830>
- Siddiquey, I. A., Ukaji, E., Furusawa, T., Sato, M., & Suzuki, N. (2007). The effects of organic surface treatment by methacryloxypropyltrimethoxysilane on the photostability of TiO<sub>2</sub>. *Materials Chemistry and Physics*, 105(2–3), 162–168. <https://doi.org/10.1016/j.matchemphys.2007.04.017>
- Silva, A. L., Salvador, G. M. da S., Castro, S. V. F., Carvalho, N. M. F., & Munoz, R. A. A. (2021). A 3D printer guide for the development and application of electrochemical cells and devices. *Frontiers in Chemistry*, 9, 684256. <https://doi.org/10.3389/fchem.2021.684256>
- Sodagar, A., Bahador, A., Khalil, S., Saffar Shahroudi, A., & Zaman Kassae, M. (2013). The effect of TiO<sub>2</sub> and SiO<sub>2</sub> nanoparticles on flexural strength of poly(methyl methacrylate) acrylic resins. *Journal of Prosthodontic Research*, 57(1), 15–19. <https://doi.org/10.1016/j.jpor.2012.05.001>
- Tham, W. L., Chow, W. S., & Ishak, Z. A. M. (2010). The effect of 3-(trimethoxysilyl) propyl methacrylate on the mechanical, thermal, and morphological properties of poly(methyl methacrylate)/hydroxyapatite composites. *Journal of Applied Polymer Science*, 118(1), 218–228. <https://doi.org/10.1002/app.32111>
- Varshney, S., Nigam, A., Pawar, S. J., & Mishra, N. (2022). Structural, optical, cytotoxic, and anti-microbial properties of amorphous silica nanoparticles synthesised via hybrid method for biomedical applications. *Materials Technology*, 37(10), 1504–1515. <https://doi.org/10.1080/10667857.2021.1959190>
- Zhang, J., & Xiao, P. (2018). 3D printing of photopolymers. *Polymer Chemistry*, 9(13), 1530–1540. <https://doi.org/10.1039/C8PY00157J>
- Zornoza-Indart, A., & López-Arce, P. (2015). Silica nanoparticles (SiO<sub>2</sub>): Influence of relative humidity in stone consolidation. *Journal of Cultural Heritage*. <https://doi.org/10.1016/j.culher.2015.06.002>